Neurochem Res (2016) 41:3192–3205
DOI 10.1007/s11064-016-2043-5

ORIGINAL PAPER

Histone Deacetylase Inhibitor RGFP109 Overcomes Temozolomide Resistance by Blocking NF-κB-Dependent Transcription in Glioblastoma Cell Lines

Zong-yang Li[1] · Qing-zhong Li[1,2] · Lei Chen[1] · Bao-dong Chen[1] · Bo Wang[1] · Xie-jun Zhang[1] · Wei-ping Li[1,2]

Received: 9 March 2016 / Revised: 16 August 2016 / Accepted: 22 August 2016 / Published online: 8 September 2016

Abstract Glioblastoma (GBM) is the most frequent and aggressive tumour in the central nervous system. Many studies have demonstrated that upregulation of the NF-κB onco-pathway is accompanied by the acquisition of Temozolomide (TMZ) resistance in GBM cells. Here, we show that RGFP109, a selective histone deacetylase (HDAC1 and HDAC3) inhibitor, overcomes TMZ resistance and downregulates the expression of NF-κB-regulated pro-survival genes in a TMZ-resistant (TR) GBM cell line. RGFP109 did not alter the phosphorylation levels of NF-κB/p65 or inhibitory κBα (IκBα). Immunofluorescence microscopy showed that RGFP109 does not block the nuclear translocation of NF-κB/p65. However, co-immunoprecipitation assays revealed that RGFP109 induces the hyperacetylation of NF-κB/p65 and histones, and blocks interactions between NF-κB/p65 and its coactivators, p300 and p300/CBP-associated factor (PCAF). These results indicate that RGFP109-mediated post-translational nuclear acetylation may be involved in the regulation of NF-κB. Electrophoretic mobility shift assays revealed that RGFP109 reduces NF-κB/p65 binding to κB-DNA and decreased the transcriptional level of κB-mediated genes, suggesting that RGFP109-induced hyperacetylation leads to attenuated transcription of the κB gene. In addition, RGFP109 elevates the expression of inhibitor of growth 4 (ING4), which is typically downregulated in GBM cells. Importantly, we found that RGFP109 enhances ING4 recognition and binding to NF-κB/p65, which may be positively correlated with reduced interactions between NF-κB/p65 and p300/PCAF, thereby effecting transcription of the κB gene. Finally, we show that knockdown of ING4 with plasmids containing pcDNA3.1-ING4 shRNA abolished the effect of RGFP109. Therefore, ING4 may act as a corepressor and facilitate RGFP109-triggered suppression of the NF-κB pathway. Taken together, our data show that RGFP109, an HDAC inhibitor, in combination with TMZ may be a therapeutic candidate for patients with temozolomide-resistant GBM.

Keywords RGFP109 · NF-κB · ING4 · Temozolomide · Histone deacetylase

Introduction

Glioblastoma (formerly known as glioblastoma multiforme; GBM) is the most frequent and aggressive type of malignant tumour found in the central nervous system (CNS) [1]. Conventional protocols for treating this disease begin with surgery on operable tumours accompanied by a combination of radiotherapy and chemotherapy, which is mainly based upon the alkylating agent, Temozolomide (TMZ). Unfortunately, the current therapeutic method provides only a modest survival improvement. Moreover, TMZ induces

Zong-yang Li and Qing-zhong Li have contributed equally to this work.

Electronic supplementary material The online version of this article (doi:10.1007/s11064-016-2043-5) contains supplementary material, which is available to authorized users.

✉ Wei-ping Li
wpli@szu.edu.cn

[1] Brain Center, Department of Neurosurgery, Shenzhen Key Laboratory of Neurosurgery, Shenzhen Second People's Hospital, The Clinical College of Anhui Medical University, Shenzhen University 1st Affiliated Hospital, 3002# Sungang Road, Futian district, Shenzhen 518035, China

[2] Shantou University Medical College, 22# Xinling Road, Shantou, Guangdong, China

multidrug resistance after long-term treatments, leading to an undesirable prognosis for the treatment regimen [2]. Some recent studies have demonstrated that the excessive and aberrant activation of nuclear factor-κB (NF-κB) plays a significant role in the development of the diffusively infiltrative nature, heterogeneity, anti-apoptotic effect and drug resistance in GBM cells, which ultimately results in the incurable features of GBMs [3, 4]. As a major onco-pathway in glioma, the levels of NF-κB activity, as assessed by serine phosphorylation, are much higher in GBM tissue compared with non-GBM tissue [5], which might induce the dysregulated transcription of various cytokines and numerous onco-proteins in the GBMs [6]. Therefore, it could be hypothesized that an agent preventing NF-κB transactivation might emerge as a component in the sensitization of glioma.

The transcription of NF-κB subunits are highly regulated by several post-translational nuclear modifications, especially acetylation, a dynamic and bidirectional process mediated via histone acetyltransferase and histone deacetylase (HDAC) enzymes [7]. In particular, acetylation affects NF-κB DNA binding and target gene specificity, control transcriptional activity, and interactions with coactivators and corepressors as well as the termination of the NF-κB response [8, 9]. During the enhancement of NF-κB transcriptional activity, phosphorylated p65 stimulates co-activators, such as CREB-binding protein (CBP), its homologue p300, and the p300/CBP-associated factor (PCAF), to reinforce acetyltransferase activity, thus strengthening the interaction with NF-κB-dependent genes expression [10, 11]. It has been proposed that the reversible acetylation of p65, which is acetylated by p300/PCAF and deacetylated by histone deacetylases (HDAC1 and HDAC3), affects the binding of p65 to κB-containing DNA and facilitates its removal or its interaction with p65 and IκBα, thus regulating the duration of the NF-κB response [12, 13]. These observations highlight the possibility that HDAC regulation might be a target for overcoming resistance in GBM cells by mediating the NF-κB transactivation. As a selective inhibitor of pimelic diphenylamide HDAC enzymes (class I), RGFP109 (N-(6-(2-aminophenylamino)-6-oxohexyl)-4-methylbenzamide) (Ki/IC50 of HDAC1 is 32 and 60 nM; Ki/IC50 of HDAC3 is 5 and 60 nM) [14] is capable of passing through the blood–brain barrier (BBB) to the CNS and improving the L-3,4-dihydroxyphenylalanine (L-DOPA)-induced dyskinetic phenotype in Parkinson's disease (PD) [15, 16]. The aim of this study was to determine whether RGFP109 would be a candidate reagent for combination therapy with TMZ for patients with temozolomide-resistant GBM and to elucidate the regulatory mechanism of RGFP109 in overcoming the NF-κB pathway.

We demonstrated that RGFP109 enhances TMZ-induced cytotoxicity and reverses TMZ-triggered responsive excitation and translation of the NF-κB pathway. Co-treatment with RGFP109 does not block the TMZ-induced transactivation and nuclear translocation of p65; however, RGFP109 can induce the hyperacetylation of p65 and histones, thereby reducing p65 binding to κB-DNA and repressing interactions between p65 and its transcriptional co-activators. This ultimately inhibits the expression of components of the NF-κB pathway. In addition, RGFP109 treatment elevates the expression of inhibitor of growth 4 (ING4), which may have a significant role in suppressing TMZ resistance by reinforcing physical interactions between ING4 and p65, thereby regulating gene expression in the NF-κB pathway.

Materials and Methods

Drugs and Reagents

Temozolomide (TMZ) for cell culture and experiments was purchased from Selleck Chemicals (Houston, TX, USA). Foetal bovine serum (FBS), heat-inactivated horse serum, penicillin and streptomycin were purchased from Gibco (Grand Island, NY, USA). Dimethylsulfoxide (DMSO), Dulbecco's Modified Eagle Medium (DMEM). The HDAC inhibitor, (RGFP109), was purchased from Selleck Chemicals (Houston, TX, USA). Cell viability was evaluated with the Cell Counting Kit-8 (CCK-8, Dojindo Molecular Technologies, Kumamoto, Japan).

Cell Lines and Culture Conditions

The human malignant glioma A172, U118, U251 and U87 cell lines, obtained from the Institute of Biochemistry and Cell Biology (Shanghai Institutes for Biological Sciences, Chinese Academy of Sciences, Shanghai, China), were cultured in DMEM supplemented with 10% heat-inactivated FBS, 100 units/ml of penicillin and 100 μg/ml of streptomycin in a humidified atmosphere containing 5% CO_2 at 37 °C. All media and sera were purchased from Gibco Life Technologies (Carlsbad, CA, USA).

To establish the Temozolomide resistant (TR) cell line, cell lines were treated with graded concentrations of TMZ from 5 to 600 μM. The resistant clones isolated by this method were denoted as TR cell lines. The parental cell lines treated with DMSO alone were included for parallel analysis.

Cell Viability Assay and Temozolomide Resistance Attenuation Analysis

Cell viability was evaluated with the Cell Counting Kit-8. Cells were plated in 96-well plates at a density of 2500 cells

per well. The cells were cultured in 100 mL of the medium containing vehicle or drugs with indicated concentration, and cells were incubated at 37 °C for indicated time points. Then, 90 μl of culture medium and 10 μl of CCK-8 solution were added to each well. The plate was maintained at 37 °C for 2 h, and the absorption was measured at 450 nm on a micro-plate reader (Spectrafluor, TECAN, Sunrise, Austria). Cell viability was presented as the percentage of survivors relative to the vehicle-treated control culture. Each sample was carried out in triplicate, and the entire experiment was repeated twice.

Annexin V/PI Double Staining

The apoptosis in GBM cells was determined by Fluorescence Activated Cell Sorter (FACS) assay via the Annexin V/PI assay kit. GBM cells were collected and incubated with Annexin V working solution and PI (1 μg/ml final concentration) for 10 min, then added 400 μl of 1× binding buffer, and then Annexin V/PI double staining was detected by a flow cytometer (BD Biosciences, CA, USA).

Measurement of DNA Fragmentation

The DNA fragmentation of apoptotic GBM cells was detected using a terminal deoxynucleotidyl transferase-mediated biotinylated UTP nick end labelling (TUNEL) kit (Roche Diagnostics Corp., IN, USA). The cells were cultured on coverslips for 24 h. At the end of the drug treatment, the cells were fixed by incubation in a 10% neutral buffered formalin solution for 30 min at room temperature. Next, the cells were incubated with a methanol solution containing 0.3% H_2O_2 for 30 min at room temperature and then incubated with a permeabilising solution (0.1% sodium citrate and 0.1% Triton X-100) for 2 min at 4 °C. The cells were incubated with the TUNEL reaction mixture for 60 min at 37 °C and visualized by inverted fluorescence microscopy (Leica, Germany). The TUNEL-positive nuclei of four non-overlapping fields per coverslip were counted, and these counts were converted to percentages by comparing the TUNEL-positive counts to the total numbers of cell nuclei, as determined by Hoechst 33,342 counterstaining.

Immunoblotting Assay

At the end of treatments, the cells were harvested and washed once with PBS. The cells for other quantities of proteins were lysed with a cell lysis buffer containing 1% phenylmethylsulfonyl fluoride (PMSF). The whole cell lysates were centrifuged at 12,000 rpm for 5 min at 4 °C and the supernatant was collected. Protein concentration was determined using the bicinchoninic acid assay. Equal amounts of protein (10 μg) were separated by electrophoresis on 10% sodium dodecyl sulfate polyacrylamide gels and transferred onto nitrocellulose membranes. These membranes were incubated with 5% (w/v) non-fat milk powder in Tris-buffered saline containing 0.1% (v/v) Tween-20 (TBST) for 40 min to block nonspecific binding sites. The membranes were then incubated overnight at 4 °C with primary antibodies. After washing with TBST, the membranes were incubated for 1 h at room temperature with the secondary antibodies. After rewashing with TBST, the bands were developed by enhanced chemiluminescence with primary antibodies obtained from the following sources: anti-GAPDH, anti-MGMT, anti-Bcl-2, anti-Bcl-x, anti-survivin, anti-ING4, anti-p300 and anti-PCAF (Santa Cruz, CA); anti-Histone H3 (acetyl K56), anti-Histone H4 (acetyl K16), anti-IκB alpha (phospho S32 + S36), anti-IκB alpha, anti-NF-κB p65 (phospho S276), anti-NF-κB p65 (phospho S536) and anti-NF-κB p65 (Abcam, CA). The secondary peroxidase-conjugated antibodies and enhanced chemiluminescence reagents were purchased from Cell Signalling Technology (Beverly, MA). Monoclonal anti-acetyl lysine antibody was purchased from Cell Signalling Technology (Beverly, MA). Class-specific IgG was used as a control in immunoprecipitation. Horizontal scanning densitometry was done on Western blots by using acquisition into Adobe PhotoShop (Adobe Systems, Inc.).

Electrophoretic Mobility Shift Assay (EMSA)

A commercial synthetic biotin-labelled, double-stranded oligonucleotide with the κB-DNA sequence was purchased from Beyotime Institute of Biotechnology. The binding activity of acetylation of p65 and κB-DNA were detected using a Light Shift Chemiluminescent EMSA kit. The nuclear extracts were incubated with the biotin-labeled oligonucleotides for 30 min at room temperature in a binding buffer containing 50 μg/ml poly (dI-dC), 5 mM $MgCl_2$, 2.5% glycerol, and 0.05% NP-40. The DNA–protein complex was separated by a 6% polyacrylamide gel at 100 V for 1 h. The separated complexes were transferred onto a nylon membrane at 380 mA for 30 min and subsequently cross-linked to the nylon membrane using UV light. The DNA–protein bands were developed by chemiluminescence.

Real-Time RT-PCR

Total RNA was isolated from cells using Trizol reagent (Invitrogen, USA). RNA samples (2 μg) were reverse-transcribed to generate first-strand cDNA. After reverse transcription using TaqMan® Reverse Transcription Kits (Applied Biosystems), 0.5 μl reverse-transcribed products were amplified with the Vii7 real-time PCR System (Applied Biosystems) in a 10 μl final reaction volume using SYBR® Green PCR Master Mix (Applied Biosystems) under the following

conditions: 30 s at 95 °C, followed by a total of 40 cycles of two temperature cycles (15 s at 95 °C and 1 min at 60 °C). Primer sequences were as follows: human Bcl-2 forward: 5′-CACAAGAGGCCAAGGCTACCT-3′ and reverse: 5′-CA GGAAAGCA GGAAGTCTCAA-3′; human Bcl-xl forward: 5′-CCATAGAGTTCCACAAAAGTATCCC-3′ and reverse: 5′-TACCTGAATGACCACCTAGAGCCT-3′; human Survivin forward: 5′-GGCCCAGTGTTTCTTCTGCTT-3′ and reverse: 5′-GCAACCGGACGAATGCTTT-3′; β-actin served as endogenous control, and the primers were forward: 5′-CAC TGTGTTGGCGTACAGGT-3′; reverse: 5′-TCATCACCAT TGGCAATGAG-3′. The Ct value was calculated by the comparative ΔΔCt method using the SDS Enterprise Database software (Applied Biosystems).

Immunofluorescence Microscopy

For immunofluorescence analysis, cells growing on glass coverslips were washed with PBS and then fixed with 4 % (w/v) paraformaldehyde for 20 min at 37 °C. The cells were washed with PBS, permeabilized with 0.1 % (v/v) Triton X-100 for 1 h, and blocked for 30 min in serum-supplemented medium. After another wash with PBS, immunostaining was performed by incubating the cells with the anti-NF-κB p65 (phospho S276), anti-NF-κB p65 (phospho S536) primary antibodies for 2 h at room temperature (25 °C). Primary antibodies were diluted in 0.1 % (v/v) Triton X-100, 0.2 % (w/v) BSA, 0.5 mM PMSF and 1 mM dithiothreitol in PBS. After washing with PBS, the bound primary antibodies were detected using FITC-conjugated goat anti-rabbit antibodies, Cy5-conjugated goat anti-mouse antibodies or Cy5-conjugated donkey anti-rabbit antibodies for 2 h at room temperature. Images were acquired using a Leica fluorescence microscope (Leica, Germany).

Transfection

U251 cells (7.5×10^5) were transfected with plasmids containing pcDNA3.1-ING4 shRNA or equivalent concentrations of control shRNA using the Gene Jammer reagent in accordance with the manufacturer's instructions. 24 h after transfection, the cells were harvested to western blotting for detecting NH2-EKQIESSDYDSSSSKGK-OH peptide of ING4.

Statistical Analysis

The results are presented as the means ± standard deviation (SD). All of the statistical analysis was performed with SPSS 17.0 software. Student's *t* test was performed, and differences were accepted as statistically significant at $P < 0.05$. All of the experiments were performed a minimum of three times.

Results

Establishment of TMZ-Resistant Cell Lines

The TMZ-resistant (TR) cell lines were generated from the TMZ-sensitive parental cell lines by initially treating the cells with a low dose of TMZ in culture media for 2 weeks, and then doubling the TMZ concentration every two passages over a period of 4–8 weeks, with the doses ranging between 5 and 600 μM. The half maximal inhibitory concentration (IC50) of TMZ-mediated growth inhibition in the resistant A172, U118, U251, U87 and the parental cell lines was determined using the CCK-8 assay. The IC50 of TMZ in the four resistant cell lines was significantly upregulated compared with the parental cell lines. The IC50 of TMZ in the TR/A172 cells was 254.33 ± 17.53 μM and, in the parental A172 cells, the IC50 was 33.91 ± 4.37 μM (Fig. 1a). The IC50 of TMZ in the TR/U118 cells was 302.77 ± 23.54 μM and, in the parental U118 cells, the IC50 was 52.13 ± 5.39 μM (Fig. 1b). The IC50 of TMZ in the TR/U251 cells was 283.45 ± 22.38 and, in the parental U251 cells, the IC50 was 39.88 ± 6.25 μM (Fig. 1c). The IC50 of TMZ in the TR/U87 cells was 323.46 ± 28.14 μM and, in the parental U87 cells, the IC50 was 66.34 ± 7.54 μM (Fig. 1d). These results show that TMZ sensitivity decreased by more than 4–6-fold in the resistant cells compared with the parental cells. In addition, the TMZ resistance of the TR cells was maintained in the absence of TMZ for approximately 2 months (data not shown).

Histone Deacetylase Inhibitor RGFP109 Enhanced TMZ-Induced Cytotoxicity in Four TMZ-Resistant Cell Lines

To determine the role of RGFP109 in restoring TMZ-induced cytotoxicity in TMZ-resistant (TR) cell lines, we established a method to assess the effect of simultaneously treating TR cells with TMZ and RGFP109. The IC50 for TMZ mediated growth inhibition in parental and TMZ-resistant cell lines were named "parental-IC50" and "TR-IC50", respectively. We treated four types of TR cells with TMZ alone at the concentration of their parental-IC50 (TR/A172, 34 μM; TR/U118, 52 μM; TR/U251, 40 μM; TR/U87, 66 μM) for 24 h. At the parental-IC50, there was no obvious cytotoxicity, and the cell survival rate of TR/A172, TR/U118, TR/U251 and TR/U87 cell lines were 97.3 ± 4.6 %, 95.8 ± 5.4 %, 94.7 ± 6.2 % and 98.3 ± 6.5 %, respectively (Fig. 2a–d). Therefore, we treated each of the TR cell lines with a combination of TMZ at the parental-IC50 and RGFP109 to determine whether RGFP109 enhances TMZ-induced cytotoxicity. We used RGFP109 at 10–120 μM because, at this concentration, RGFP109 alone showed no obvious dosage- or time-dependent cytotoxicity (Fig. 2a–h).

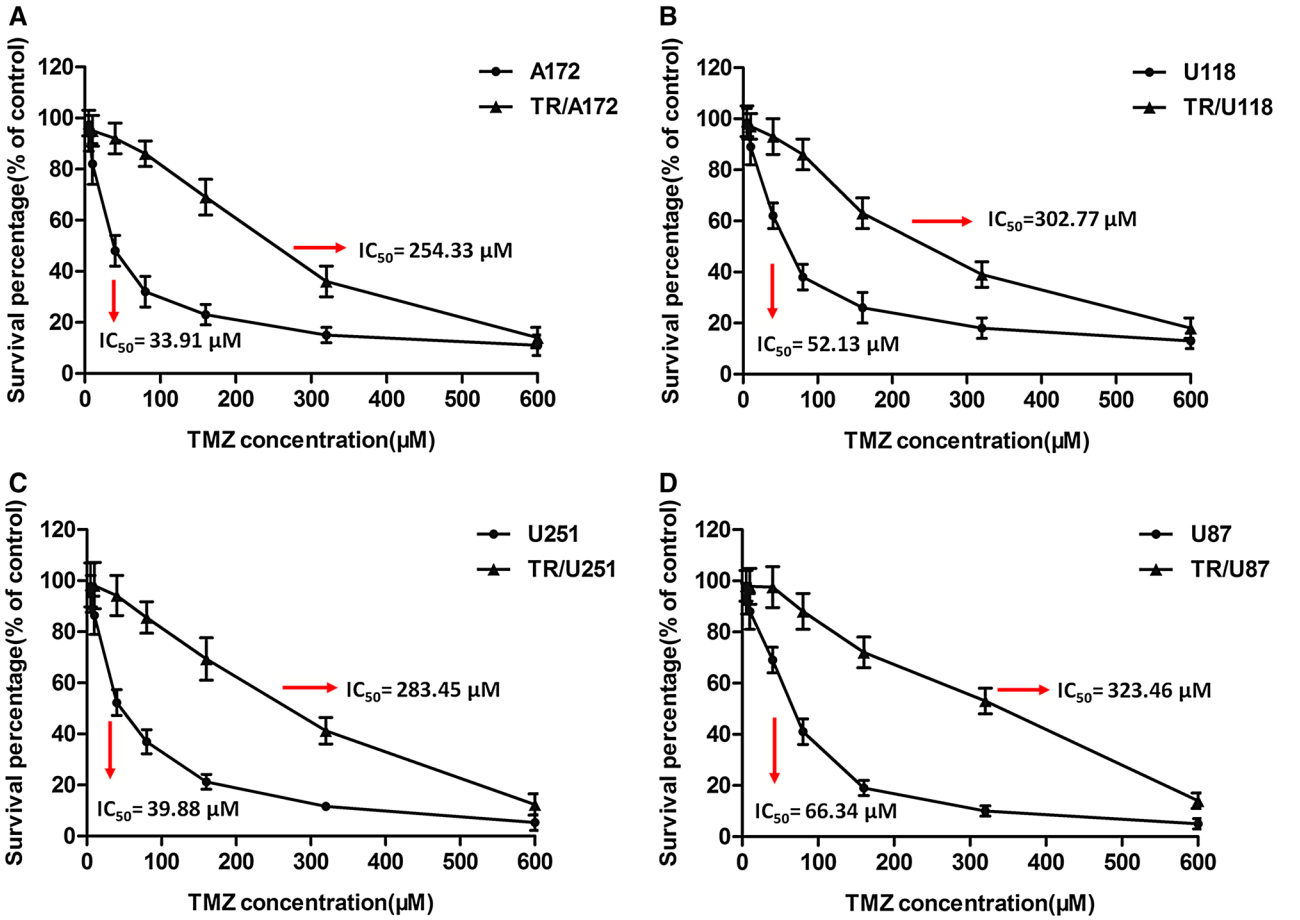

Fig. 1 Establishment of TMZ-resistant (TR) GBM cell lines. **a–d** Evaluation of temozolomide resistance in four glioblastoma cell lines. Cells were cultured in the presence of 5–600 μM of TMZ. A dose-dependent association between the survival rate of cells and TMZ concentration can be observed. Each group was cultured for 24 h in the presence of different concentrations of TMZ, followed by an evaluation of IC50 for TMZ inhibited growth in A172-TR/A172, U118-TR/U118, U251-TR/U251 and U87-TR/U87

The dosage of RGFP109 that made the parental-IC50 of TMZ produce the half maximal inhibitory effect (generating the same cytotoxicity of TR-IC50) in TR cell lines was designated as the "TMZ Combination Concentration (TCC)". At this concentration, RGGP109 attenuates TMZ resistance and restores TR cells to parental cell levels of chemosensitivity to TMZ.

Cell viability assays demonstrated that RGFP109 significantly increased TMZ-induced cytotoxicity in four TMZ-resistant cell lines. Figure 2a–d show that the TCCs of RGFP109 in TR/A172, TR/U118, TR/U251 and TR/U87 cells were 47.6 ± 4.80 μM, 54.6 ± 4.20 μM, 42.1 ± 3.70 μM and 62.3 ± 4.80 μM, respectively. As the contrast, we repeated cell viability assays with Panobinostat in four TR cell lines, and confirmed sensitizing effect of HDACs inhibition (Fig. Supplemental data 1). Furthermore, co-treatment with RGFP109 (TCC) and TMZ (parental-IC50) inhibited cell survival in a time-dependent manner for 0–48 h. Cells exposed to RGFP109 (TCC) alone showed no obvious time-dependent cytotoxicity for 0–48 h (Fig. 2e–h). These pharmacodynamics assays of the four GBM cell lines show that RGFP109 displayed the same effect of sensitization and that the TR/U251 cells showed the lowest TCC. Therefore, the TR/U251 cell line was selected for investigating the mechanism underlying RGFP109-mediated enhancement of TMZ-induced cytotoxicity.

Combined Treatment with RGFP109 Lead to Apoptosis of TR/U251 Cells as Determined by FACS and TUNEL Assays

To confirm and better quantify cytotoxicity and apoptosis induced by the combination treatments, as observed in the CCK-8 assays, we determined the percentage of apoptotic cells by annexin V/PI double staining and flow cytometry. The DNA fragmentation in the apoptotic cells was examined by TUNEL. There was a significant increase in TR/U251 cells with Annexin V+/PI- and Annexin V+/PI+ after treatment with a combination of TMZ and RGFP109 for 24 h compared with control and TMZ alone groups.

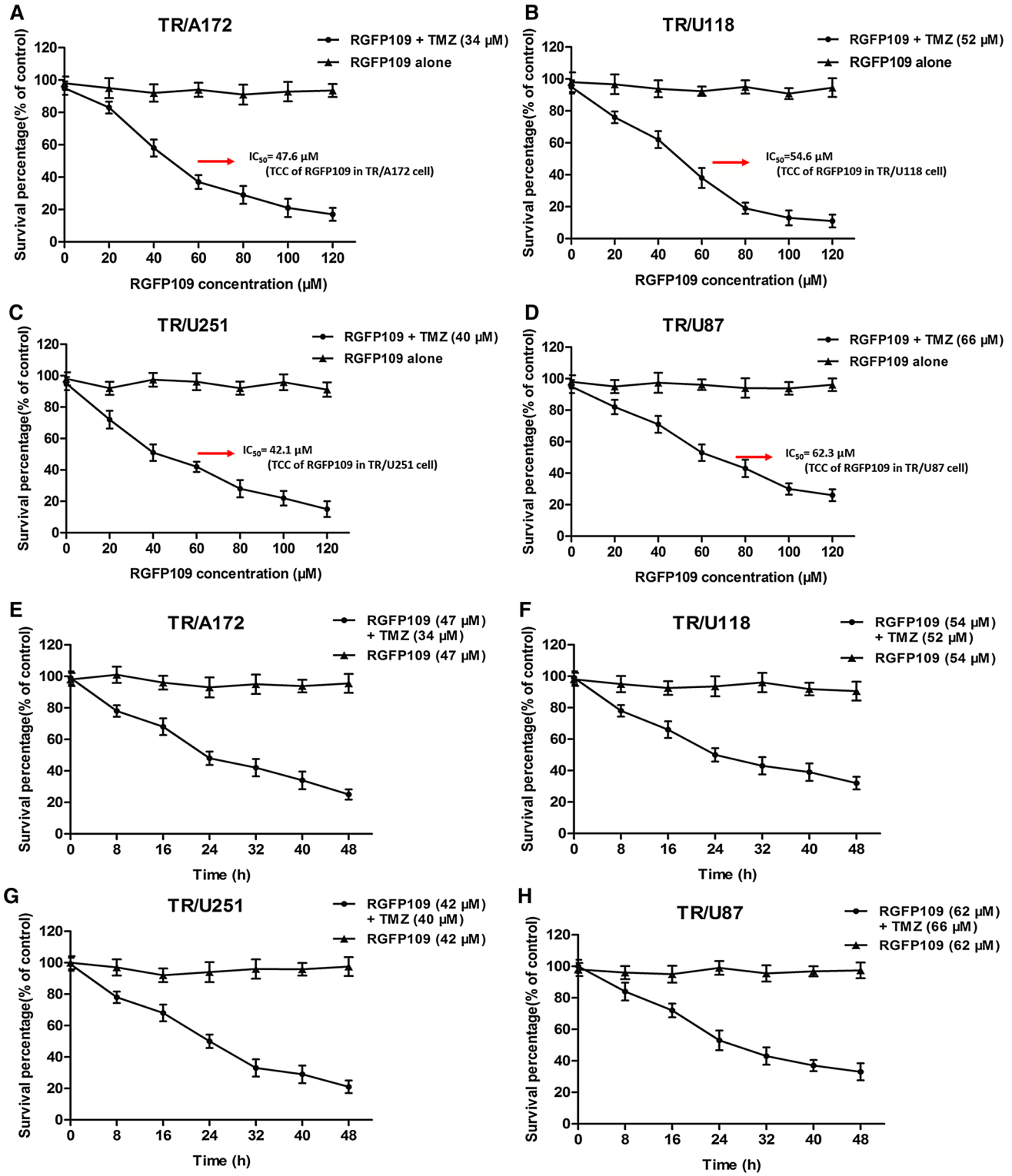

Fig. 2 RGFP109 enhanced TMZ-induced cytotoxicity in TR cells. **a**–**d** Each group was cultured for 24 h in different concentrations of RGFP109 and TMZ. Cell viability rates were determined in four TR cell lines. Treatment with RGFP109 markedly enhanced TMZ-decreased cell viability, while treatment with RGFP109 (10–120 μM) alone showed no obvious cytotoxicity. **e**–**h** Evaluation of cell viability to determine time-dependent effects (0–48 h) from simultaneous treatment of RGFP109 and TMZ. Data were collected for the concentrations of RGFP109 and TMZ at the time points indicated. Cell survival was inhibited in a time-dependent manner for 0–48 h by co-treatment with RGFP109 and TMZ, while the RGFP109 alone exerted no time-dependent effects. *TMZ* Temozolomide, *TR* TMZ-resistant, *TCC* TMZ Combination Concentration

Apoptosis in the combination treatment group was at 38.79 %, a significant increase compared with the control group (**P < 0.001), while the percentage of apoptotic cells in control and TMZ alone groups showed no obvious up-regulation (Fig. 3a, c), suggesting that RGFP109 enhanced cytotoxicity in TR/U251. TR/U251 cells treated with a combination of TMZ and RGFP109 for 24 h displayed a significant increase in TUNEL-positive cells, to 46.2 % of the total cell number (**P < 0.001), while only 2.54 % of the control cells and 4.82 % of TMZ treated cells were TUNEL-positive (Fig. 3b, d).

NF-κB and NF-κB-Regulated Genes MGMT, Survivin, Bcl-2 and Bcl-x are Constitutively Activated in TR/U251 Cells

The constitutive activation of NF-κB has been a major cause of apoptotic resistance in GBM cells; therefore, we examined the activation of NF-κB in TR/U251 cells compared with parental cells. We analysed the levels of total and phosphorylated p65 (p-p65) in TR/U251 and parental cells by immunoblotting with antibodies specific for p-p65 (S276) and (S536). When compared to parental cells, which displayed very low levels of p-p65, TR/U251 cells displayed elevated levels of p-p65 (S276) and p-p65 (S536). NF-κB activation was confirmed by measuring the levels of total and phosphorylated IκBα (p-IκBα). In TR/U251 cells, the level of p-IκBα was elevated compared with the parental cells. Accordingly, Fig. 3e shows that TMZ resistant cells display increased levels and activation of NF-κB, which may be associated with the apoptotic resistance acquired by TR cells. To confirm that the up-regulation of NF-κB was positively correlated with TMZ resistance and anti-apoptotic activity in TR cells, we analysed the expression of NF-κB-related genes, MGMT, Bcl-2 and Bcl-x. Western blot analysis detected high levels of MGMT, Bcl-2 and Bcl-x in TR/U251 cells compared with the parental cells. These data suggested that, in TR cells, the levels of MGMT, survivin, Bcl-2 and Bcl-x expression are elevated, (Fig. 3f), coinciding with NF-κB activation and implying

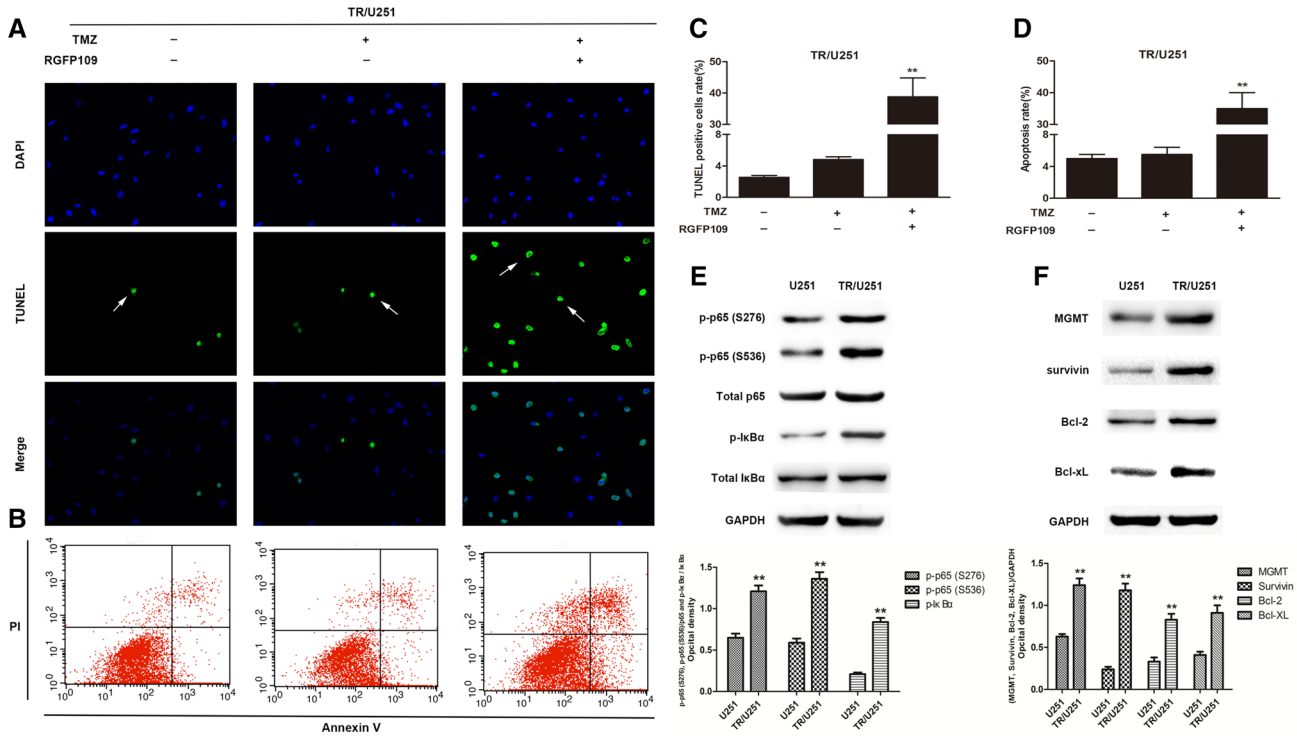

Fig. 3 Effects of combined treatment with RGFP109 and TMZ on apoptosis and the expression of NF-κB and NF-κB-regulated genes in TR/U251 cells. **a** Cell apoptosis was determined by Annexin V-PI double staining kits and flow cytometry. **b** Quantification of the apoptosis. TUNEL staining, **c** Representative images of TUNEL-positive cells (*green, top* row) and Hoechst counterstaining (*blue, middle* row). **d** Quantification of TUNEL staining. The histogram shows the relative proportion of TUNEL-positive cells in different treatment groups. **e** Levels of p-p65 (S276) and (S536) were elevated in TR/U251 cells and reduced in the parental U251 cells. In addition, p-IκBα expression was stronger in TR/U251 cells than in parental U251 cells, indicating that the NF-κB pathway was stimulated in the resistant cell line. **f** Western blot analysis also detected high levels of MGMT, survivin, Bcl-2 and Bcl-x in TR/U251 cells compared with the parental cells, demonstrating that NF-κB-regulated genes are constitutively activated in TR/U251 cells. The results are expressed as the means ± SD of three independent experiments. *Significant difference from the parental U251 cells (P < 0.05). **Significant difference from the parental U251 cells (P < 0.01). (Color figure online)

that these anti-apoptotic proteins may be associated with TMZ resistance.

RGFP109 Down-Regulated NF-κB-Regulated Genes, but did not Alter the Activation or Nuclear Translocalization of p65 in TR/U251 Cells

To explore the molecular mechanisms underlying RGFP109-mediated enhancement of TMZ-induced cell death in TR/U251 cells, we investigated whether RGFP109 effected the expression of MGMT and other anti-apoptotic proteins in TR cells. Western blot analyses (Fig. 4a) revealed that treatment with TMZ and RGFP109 significantly reduced the levels of MGMT, survivin, Bcl-2 and Bcl-x in TR/U251 cells compared with the control and TMZ alone treatment groups. These data support a potential association between RGFP109-mediated enhancement of TMZ-induced cytotoxicity and the expression of pro-survival proteins during the reversion of TMZ resistance.

The expression levels of MGMT, Bcl-2 and Bcl-x were regulated and consistent with the activation of NF-κB, which is upstream of these anti-apoptotic proteins. Therefore, we investigated whether the inhibition of NF-κB coincides with the down-regulation of pro-survival proteins, contributing to RGFP109-mediated reversion of TMZ resistance. Unexpectedly, treatment with RGFP109 failed to decrease the levels of p-p65 (S276) and p-p65 (S536) in TR/U251 cells (Fig. 4b). Furthermore, treatment with RGFP109 did not alter the expression of phosphorylated IκBα (p-IκBα). Because the activation of NF-κB is accompanied by the translocation of activated dimers to the nucleus and binding to κB elements, we simultaneously evaluated the expression and distribution of total p65, p-p65 (S276) and p-p65 (S536) by indirect immunofluorescence. As shown in Fig. 4c, in the absence of stimuli, p65 is predominantly cytoplasmic with moderate levels of nuclear p-p65 (S276) and p-p65 (S536). Upon stimulation with TMZ and RGFP109, p65 aggregates and accumulates in the nucleus, and levels of p-p65 (S276) and p-p65 (S536) are elevated, indicating that treatment with RGFP109 does not block the activation and nuclear translocalization of p65.

RGFP109 Induced Hyperacetylation of p65 and Histones

It was recently reported that the class I subfamily of HDACs, involved in the acetylation of p65 and histones, can activate the NF-κB pathway. Therefore, we investigated whether treatment with RGFP109 could initiate the hyperacetylation of p65 and histones. Analyses by immunoprecipitation indicated that the simultaneous treatment of cells with TMZ and RGFP109 enhanced the level of acetylated lysine residues in p65 compared with the control and TMZ groups alone (Fig. 5a). Furthermore, treating cell cultures with TMZ and RGFP109 triggered hyperactive histone acetylation, which was analysed by immunoblotting with antibodies specific for acetylated histones 3 (Ac-H3) and acetylated histones 4 (Ac-H4). In the absence of RGFP109 (Fig. 5a), treatment with TMZ alone induced low levels of Ac-H3 and Ac-H4 compared with the control group, while simultaneous treatment with TMZ and RGFP109 caused an up-regulation in the levels of Ac-H3 and Ac-H4. These results imply a tight regulation of p65 and histones acetylation by deacetylases. Furthermore, RGFP109-induced hyperacetylation may repress NF-κB dependent transcription because p65 contains the transcriptional activation domain.

Hyperacetylation of p65 Reduced the Binding to κB-DNA and κB-Mediated Genes Transcription

Acetyl-acceptor lysines 122 and 123 are the only p65 residues involved in DNA binding. In this study, we used EMSA to show that the acetylation of p65 may affect its interaction with κB-DNA. Acetylation of FLAG-p65 reduced its ability to bind κB-DNA (Fig. 5b). Wild type p65 and the KK-RR mutant bound to the κB gene with similar affinities, while the KK-AA mutant could not bind to the gene (Fig. 5b). Thus, consistent with predictions from crystal structure analysis, the acetyl acceptor lysines 122 and 123 participate in high affinity binding of p65 to the κB gene. In addition, RT-PCR analysis was further performed to examine the effect of acetylation on transcriptional level of κB-target genes such as Bcl-2, Bcl-xl and Survivin in TR/U251 cells. In the absence of RGFP109 (Fig. 5b), treatment with TMZ alone did not changed the expression of Bcl-2, Bcl-xl and Survivin compared with the control group, while simultaneous treatment with TMZ and RGFP109 induced an significantly down-regulation in the mRNA levels of Bcl-2, Bcl-xl and Survivin compared with the control group. These results confirmed hyperacetylation of p65 reduced the binding to κB-DNA and decreased the transcriptional level of κB-target genes.

RGFP109 Repressed Interactions Between p65 and its Transcriptional Coactivators

Transcriptional activity of NF-κB is increased by the recruitment of transcriptional coactivators such as p300/CBP and PCAF. These coactivators stimulate localized chromatin remodelling via intrinsic histone-directed acetylation activities, enhancing p65-mediated transcription. To investigate whether RGFP109-induced hyperacetylation of p65 was involved in inhibition of the NF-κB pathway, we determined the levels of binding between p65 and its coactivators following treatment with RGFP109. Immunoprecipitation analysis (Fig. 5c) demonstrated that the

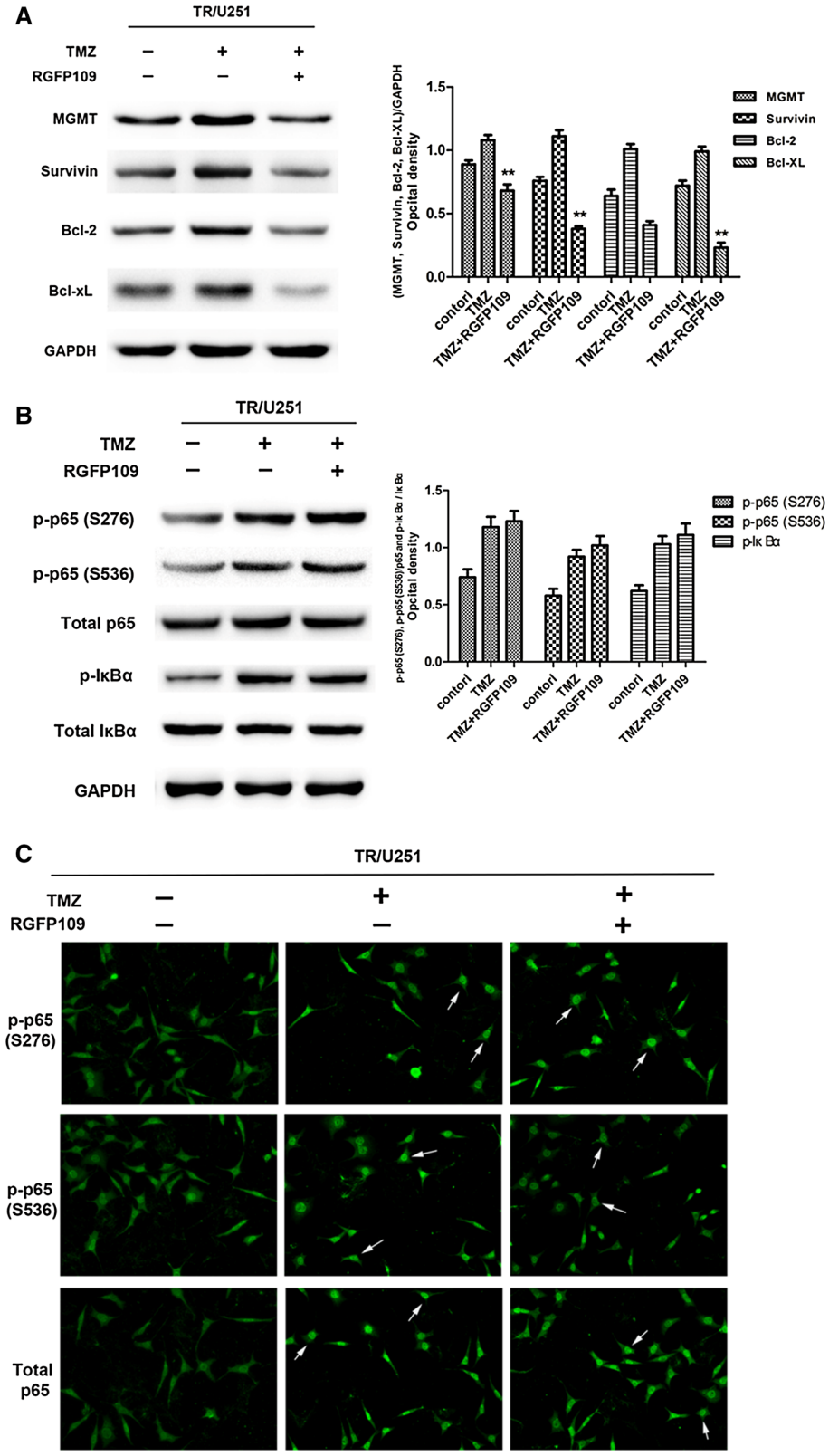

Fig. 4 RGFP109 down-regulated NF-κB-regulated genes, but did not alter the activation or nuclear translocalization of p65. **a** Expression of the NF-κB-regulated genes, MGMT, survivin, Bcl-2 and Bcl-x, were significantly reduced in TR/U251 cells by combined treatment with TMZ and RGFP109 compared with the control and TMZ alone treatment groups. **b** The levels of p-p65 (S276), p-p65 (S536) and p-IκBα were detected. Co-treatment with RGFP109 did not decrease the levels of p-p65 (S276), p-p65 (S536) and p-IκBα in TR/U251 cells. The results are expressed as the means ± SD of three independent experiments. *Significant difference from the TMZ treatment alone ($P < 0.05$). **Significant difference from the TMZ treatment alone ($P < 0.01$). **c** Immunofluorescence data on the expression and distribution of total p65, p-p65 (S276) and p-p65 (S536). *Arrows* indicate cells with p65 nuclear translocation. Treatment with RGFP109 did not affect the nuclear translocalization of p65

simultaneous treatment of cells with TMZ and RGFP109 attenuated p65-p300 and p65-PCAF interactions, while the expression levels of p300 and PCAF were not altered. These results suggest that RGFP109 did not down-regulate the levels of p300 and PCAF, but that the RGFP109-induced hyperacetylation of p65 might block the binding of p65 to its coactivators to reinforce the p65-mediated transcription.

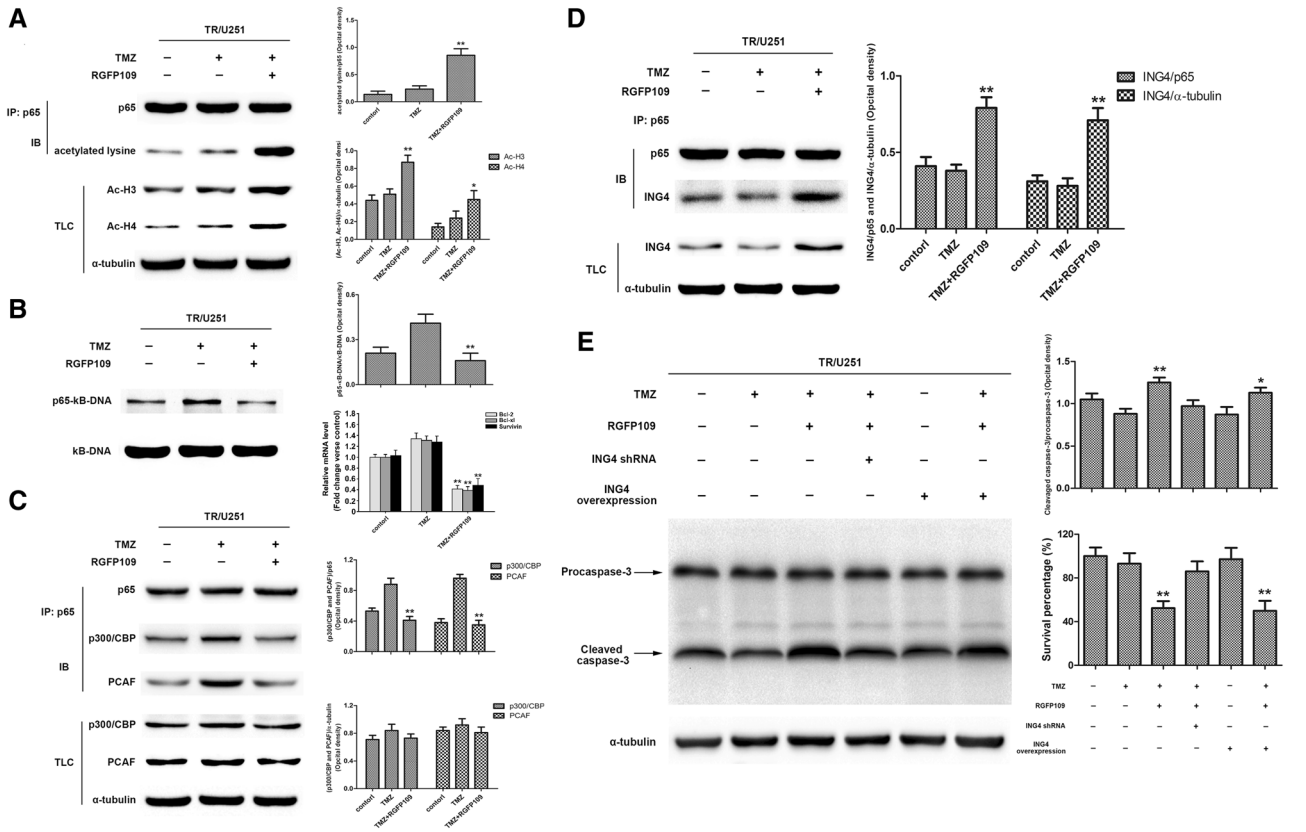

Fig. 5 RGFP109-induced hyperacetylation of p65 and histones, which reduced the binding of p65 with the κB gene, and repressed interactions between p65 and its transcriptional coactivators. Furthermore, RGFP109 increased interactions between ING4 and p65. ING4 contributed to the RGFP109-induced TMZ cytotoxicity. **a** Detecting levels of acetylated p65 and histones. Immunoprecipitation analysis revealed that the simultaneous treatment of cells with TMZ and RGFP109 increased the levels of p65 with acetylated lysine residues and up regulated levels of Ac-H3 and Ac-H4. **b** Detecting DNA binding to p65 and κB-mediated genes transcription. Acetylation of FLAG-p65 reduces its ability to bind the κB gene. To determine whether the acetylated p65 still interacts with the κB gene, binding activity was determined by EMSA. Effect of acetylation on transcriptional level of κB-target genes was detected by real-time RT-PCR. **c** Immunoprecipitation analysis determined the levels of binding between p65 and its coactivators. The results demonstrate the simultaneous treatment of cells with TMZ and RGFP109 attenuated the p65-p300 and p65-PCAF interactions, while the expression levels of p300 and PCAF were not altered. The results are expressed as the means ± SD of three independent experiments. *Significant difference from the TMZ treatment alone ($P < 0.05$). **Significant difference from the TMZ treatment alone ($P < 0.01$). **d** Detecting ING4 levels and binding with p65. RGFP109 elevated the ING4 levels and immunoprecipitation experiments confirmed that RGFP109 increased physical interactions between ING4 and p65. **e** Evaluating the effect of ING4 in improving the RGFP109-enhanced TMZ cytotoxicity. Knockdown of ING4 decreased the cleavage of caspase-3, indicating attenuation of RGFP109-enhanced TMZ cytotoxicity, while overexpressing ING4 alone did not alter TMZ-induced cytotoxicity compared with wild-type TR/U251 cells. The results are expressed as the means ± SD of three independent experiments. *Significant difference from the TMZ treatment alone, ING4 knockdown and overexpressing ING4 alone group ($P < 0.05$). **Significant difference from the TMZ treatment alone ($P < 0.01$)

RGFP109 Increased Interaction Between ING4 and p65

Many reports have suggested that ING4 suppresses tumourigenesis by regulating the activity of NF-κB, which is maintained at low levels or is absent in human glioma [5, 17, 18]. Therefore, to determine whether the RGFP109-induced TMZ cytotoxicity is linked to ING4, we performed immunoblot analyses to determine ING4 protein expression in different treatment groups. As shown in Fig. 5d, RGFP109 elevated the levels of ING4 compared with the control and TMZ alone treatment groups. To confirm the interaction between ING4 and p65 after the treatment with RGFP109, immunoprecipitation experiments were conducted with antibodies against p65, and immunoprecipitated proteins were detected by western blot using antibodies against ING4 protein. The results confirmed that RGFP109 stimulated the physical interaction between ING4 and p65 compared with the control and TMZ alone treatment groups (Fig. 5d).

ING4 Contributed to the RGFP109-Enhanced TMZ Cytotoxicity

To confirm the possible role of ING4 in RGFP109-enhanced TMZ cytotoxicity, we investigated whether ING4

knockdown or overexpression would alter the therapeutic efficacy of RGFP109 and TMZ in TR/U251 and TR/U87 cells. The results showed that cells in which ING4 was depleted by shRNA were resistant to combined treatment with RGFP109 and TMZ compared with wild-type cells, which exhibited vulnerability to drugs (Fig. 5e). Overexpression of ING4 did not alter the viability of RGFP109-treated cells and there was no significant increase in TMZ cytotoxicity compared with wild-type cells. Furthermore, in the absence of RGFP109, overexpressing ING4 alone did not enhance TMZ-induced cytotoxicity (Fig. 5e). These results suggest that ING4 is not sufficient to abolish TMZ resistance, despite having a crucial role in RGFP109-enhanced TMZ cytotoxicity.

Discussion

Our results reveal that RRGFP109, a selective inhibitor of HDACs (class I, HDAC1 and 3), can overcome TMZ resistance via the post-induction suppression of NF-κB-mediated transcription. This is consistent with studies showing that abnormal activation of NF-κB and relevant onco-suppressor genes are conducive to TMZ resistance [3]. As a transcriptional factor, the activity of NF-κB undergoes a number of post-induction modifications that cause crucial shifts in its physical interactions with other NF-κB proteins, transcriptional coactivators and the κB genes [19]. The reversible process of post-induction acetylation, where acetyl groups are enzymatically placed onto the lysine residues of target proteins, is a significant event in the transactivation of NF-κB during stimulation [12, 13]. Therefore, we focused our research on HDAC-mediated regulation of the NF-κB pathway, which might be a potential target for reversing TMZ resistance in GBM cells. HDACs belong to an evolutionarily conserved family of proteins that catalyse the post-translational modification of histones by removing acetyl groups from lysine side chains [20]. Recently, several proteomic studies have confirmed that the canonical function of these enzymes in the regulation of histones represents only a fraction of the properties of HDACs. Furthermore, there is a growing list of "non-histone" substrates that are positively correlated to the biological activity of HDACs, which implies the existence of a great diversity of unexplored HDAC-dependent mechanisms that may be pharmacological targets [21, 22].

We established the TR GBM cell lines (Fig. 1) and a method to assess the effect of treating TR cells simultaneously with TMZ and RGFP109. We demonstrated that RGFP109, a selective inhibitor of HDACs (HDAC1 and HDAC3) [23], attenuates TMZ resistance and enhances TMZ-induced cytotoxicity in TR/A172, TR/U118, TR/U251 and TR/U87 cell lines, while the treatment with RGFP109 (10–120 μM) alone showed no obvious dosage- or time-dependent cytotoxicity (Fig. 2). We determined the "TCC", the concentration of RGFP109 that increases TR cell chemosensitivity to that of the parental cells, and showed that TR/U251 cells had the lowest TCC. Therefore, we chose the TR/U251 cells for additional research on the mechanism of RGFP109 action. We confirmed that RGFP109 induces sensitization using FACS and TUNEL assays (Fig. 3a–d), and found elevated levels of p-p65 (S276), p-p65 (S536), p-IκBα and NF-κB-regulated pro-survival genes in TR/U251 cells compared with the parental U251 cells (Fig. 3e, f). These data suggest that NF-κB-induced anti-apoptotic proteins may cause TMZ resistance. Subsequently, we determined that RGFP109 dramatically decreased overexpression of the NF-κB regulated anti-apoptotic proteins, MGMT, survivin, Bcl-2 and Bcl-x in TR/U251 cells (Fig. 4a). To ascertain how RGFP109 counteracts drug resistance and whether modulation of the NF-κB pathway is involved in RGFP109-induced TMZ cytotoxicity, we investigated the mechanism by which RGFP109 attenuates NF-κB-mediated gene expression. Interestingly, the data in Fig. 4b shows that combined treatment with RGFP109 did not decrease the level of p-p65 or alter the expression of p-IκBα. Immunofluorescence assays revealed that RGFP109 does not block TMZ-induced aggregation and accumulation of p-65 in the nucleus (Fig. 4c). When stimulated, activated NF-κB translocates and accumulates in the nucleus. Therefore, our data eliminates the possibility that RGFP109 suppresses the NF-κB pathway by disrupting the IKK complex-dependent excitation and translocation of NF-κB proteins [24]. This suggests that the function of NF-κB complexes is controlled by RGFP109-mediated modifications in the nucleus, which eventually regulate transcriptional activity, DNA binding and target gene specificity. Our findings also show that RGFP109 triggers the hyperacetylation of p65 and histones (Fig. 5a). Elevated levels of p65 with acetylated lysine residues were detected by immunoprecipitation assays, and hyperactive histone acetylation was detected using antibodies specific for Ac-H3 and Ac-H4. Because p65 contains the transcriptional activation domain, the reversible acetylation of p65 is critical during post-induction modifications [25]. Additionally, differences in the number and sites of acetylation cause the multiple distinct effects of p65 [26, 27]. These results led us to hypothesize that hyperacetylation would lead to decreased levels of DNA-bound p65, directly disrupting p65-dependent transcription of the κB gene. The data shown in Fig. 5b demonstrate that hyperacetylation of p65 reduces interaction with the κB gene, thereby decreasing the transcriptional level of κB-target genes such as Bcl-2, Bcl-xl and Survivin. Additional analyses in TR/U251 cells demonstrated that RGFP109 does not down-regulate the levels of p300 and PCAF, instead it blocks p65 from binding to its coactivators (Fig. 5c). Under normal circumstances, NF-κB

is regulated post-induction by transcriptional coactivators that mediate crucial transcriptional process and assist in nuclear modifications via their intrinsic histone acetyltransferase (HAT) activity [28, 29]. Enhancement of NF-κB transcriptional activity requires recruitment of these coactivators and the acetyltransferase activity of CBP/p300 and PCAF [10]. These results suggest that RGFP109-induced hyperacetylation of p65 might prevent modifications mediated by coactivators' HAT activity because all of the p65 lysine residues could be acetylated. Hence, the HAT activity of coactivators loses selectivity and can no longer facilitate p65-mediated transcription. Conversely, the unaltered levels of p300 and PCAF suggest that RGFP109 does not prevent p65 from recruiting the coactivators that induce localized chromatin remodelling via intrinsic histone-directed acetylation activities, thereby enhancing p65-mediated transcription. This raises the possibility that RGFP109-induced hyperacetylation of histones provides a synergistic target for NF-κB mediated nuclear modifications. However, we are unable to confirm a precise mechanism and it remains unclear whether histone hyperacetylation plays a role in the interaction of p65 with the κB genes and its coactivators. Notably, during histone modification, reversible acetylation and deacetylation of the ε-amino group of lysine side chains within the N-terminal tails of histones emerged as a central regulator of DNA transcriptional programming [30]. Generally, elevated levels of histone acetylation contribute to relaxation of nucleosome, thus promoting gene transcription [31]. The inhibition of HDACs blocks DNA binding and impairs cell cycling, which is relevant for anti-cancer research [32, 33]. Therefore, RGFP109-induced hyperacetylation of histones may have diverse roles in this process. We also showed that RGFP109 elevates the level of inhibitor of growth 4 (ING4), which may be a responsible for the recruitment of coactivators and the hyperacetylation of histones [34, 35].

ING4 is a member of the ING tumour suppressor family, which includes ING1, ING2, ING3, and ING5. This family of genes suppresses tumourigenesis by regulating gene expression via binding H3-Me3K4 and recruiting HDAC1 containing complexes to nearby promoters [36–38]. ING4 interacts with coactivators, such as p300 and HBO1, to regulate histone acetyltransferase and interfere with transcription factors, including p53 and NF-κB [17, 39–41]. Nevertheless, ING4 expression is reduced in several cancers, especially in GBM cells [17, 42]. To investigate a possible mechanism for the effect of combined treatment with GBM with RGFP109 as therapy for TMZ-resistance, we examined the expression of ING4 and its interaction with p65. As shown in Fig. 5a, RGFP109 elevated the level of ING4 in TR/U251 cells compared with control and TMZ alone treatment groups, and immunoprecipitation experiments confirmed that RGFP109 enhances physical interaction between ING4 and p65. These data suggest that ING4 activation contributes to RGFP109-enhanced TMZ cytotoxicity. To confirm the role of ING4, we investigated the consequence of ING4 knockdown or overexpression during the combined treatment with RGFP109. Depleting ING4 with shRNA increased cellular tolerance to drugs compared with wild-type cells. Furthermore, overexpressing ING4 alone did not enhance TMZ-induced cytotoxicity (Fig. 5e). These data confirm that ING4 alone is not sufficient to abolish TMZ resistance in TR/U251 cells, but it does have an indispensable role in RGFP109-induced TMZ cytotoxicity.

Although, we do not understand how RGFP109 increases the level of ING4 or the mechanism by which ING4 attenuates NF-κB-mediated gene expression, this study suggests that the RGFP109 causes hyperacetylation of p65, directly blocking nuclear modifications and binding with κB-DNA, thus attenuating transcription. In addition, RGFP109-induced hyperacetylation of histones may disrupt chromatin remodelling, resulting in abnormal nucleosome relaxation and increased gene transcription leading to the compensatorily increased levels of ING4. Then, increased ING4 recognized and simultaneously bound to p65 molecules that were adjacently detained to the κB gene. Through these interactions, ING4 reduced p65-p300 and p65-PCAF interactions, thereby intervening in the transcription of NF-κB. This may be the reason why the ING4 knockdown in TR cells reversed RGFP109-enhanced TMZ cytotoxicity. Nevertheless, in the absence of RGFP109-induced hyperacetylation, ING4 cannot directly block p65 from binding to κB-DNA and relevant coactivators; the established TMZ-resistant GBM cells would regulate the nuclear modifications to cause an excessive activation of oncogenes that could encourage the events and generate the complementary pathway, which ultimately counteracted ING4-induced anti-cancer function. It may also explain why overexpressing ING4 alone did not enhance TMZ-induced cytotoxicity in TR cells.

Conclusion

This study concludes that the histone deacetylase inhibitor RGFP109 overcomes TMZ resistance by inhibiting NF-κB-dependent transcription. Our study also suggests that regulating HDACs via ING4 and the NF-κB pathway may provide a therapeutic target for GBM.

References

1. Stewart LA (2002) Chemotherapy in adult high-grade glioma: a systematic review and meta-analysis of individual patient data from 12 randomised trials. The Lancet 359:1011–1018

2. Kokkinakis DM, Bocangel DB, Schold SC, Moschel RC, Pegg AE (2001) Thresholds of O6-alkylguanine-DNA alkyltransferase which confer significant resistance of human glial tumor xenografts to treatment with 1,3-bis(2-chloroethyl)-1-nitrosourea or temozolomide. Clin Cancer Res 7:421–428
3. Bredel M, Bredel C, Juric D, Duran GE, Yu RX, Harsh GR, Vogel H, Recht LD, Scheck AC, Sikic BI (2006) Tumor necrosis factor-alpha-induced protein 3 as a putative regulator of nuclear factor-κB-mediated resistance to O6-alkylating agents in human glioblastomas. J Clin Oncol 24:274–287
4. Atkinson GP, Nozell SE, Benveniste ET (2010) NF-κB and STAT3 signaling in glioma: targets for future therapies. Expert Rev Neurother 10:575–586
5. Nozell S, Laver T, Moseley D, Nowoslawski L, De Vos M, Atkinson GP, Harrison K, Nabors LB, Benveniste EN (2008) The ING4 tumor suppressor attenuates NF-κB activity at the promoters of target genes. Mol Cell Biol 28:6632–6645
6. Kapoor GS, Zhan Y, Johnson GR, O'Rourke DM (2004) Distinct domains in the SHP-2 phosphatase differentially regulate epidermal growth factor receptor/NF-κB activation through Gab1 in glioblastoma cells. Mol Cell Biol 24:823–836
7. Greene WC, Chen LF (2004) Regulation of NF-κB action by reversible acetylation. Novartis Found Symp 259:208–217 (**discussion 218–225**)
8. Vermeulen L, De Wilde G, Van Damme P, Berghe WV, Haegeman G (2003) Transcriptional activation of the NF-κB p65 subunit by mitogen- and stress-activated protein kinase-1 (MSK1). EMBO J 22:1313–1324
9. Perkins ND, Gilmore TD (2006) Good cop, bad cop: the different faces of NF-κB. Cell Death Differ 13:759–772
10. Sheppard KA, Rose DW, Haque ZK, Kurokawa R, McInerney E, Westin S, Thanos D, Rosenfeld MG, Glass CK, Collins T (1999) Transcriptional activation by NF-κB requires multiple coactivators. Mol Cell Biol 19:6367–6378
11. Zhong H, Voll RE, Ghosh S (1998) Phosphorylation of NF-κB p65 by PKA stimulates transcriptional activity by promoting a novel bivalent interaction with the coactivator CBP/p300. Mol Cell 1:661–671
12. Chen L, Fischle W, Verdin E, Greene WC (2001) Duration of nuclear NF-κB action regulated by reversible acetylation. Science 293:1653–1657
13. Kiernan R, Bres V, Ng RW, Coudart MP, El Messaoudi S, Sardet C, Jin DY, Emiliani S, Benkirane M (2003) Post-activation turn-off of NF-κB-dependent transcription is regulated by acetylation of p65. J Biol Chem 278:2758–2766
14. Saito A, Yamashita T, Mariko Y, Nosaka Y, Tsuchiya K, Ando T, Suzuki T, Tsuruo T, Nakanishi O (1999) A synthetic inhibitor of histone deacetylase, MS-27-275, with marked in vivo antitumor activity against human tumors. Proc Natl Acad Sci USA 96:4592–4597
15. Malvaez M, McQuown SC, Rogge GA, Astarabadi M, Jacques V, Carreiro S, Rusche JR, Wood MA (2013) HDAC3-selective inhibitor enhances extinction of cocaine-seeking behavior in a persistent manner. Proc Natl Acad Sci USA 110:2647–2652
16. Johnston TH, Huot P, Damude S, Fox SH, Jones SW, Rusche JR, Brotchie JM (2013) RGFP109, a histone deacetylase inhibitor attenuates L-DOPA-induced dyskinesia in the MPTP-lesioned marmoset: a proof-of-concept study. Parkinsonism Relat Disord 19:260–264
17. Garkavtsev I, Kozin SV, Chernova O, Xu L, Winkler F, Brown E, Barnett GH, Jain RK (2004) The candidate tumour suppressor protein ING4 regulates brain tumour growth and angiogenesis. Nature 428:328–332
18. Liu E, Wu J, Cao W, Zhang J, Liu W, Jiang X, Zhang X (2007) Curcumin induces G2/M cell cycle arrest in a p53-dependent manner and upregulates ING4 expression in human glioma. J Neurooncol 85:263–270
19. Perkins ND (2006) Post-translational modifications regulating the activity and function of the nuclear factor κB pathway. Oncogene 25:6717–6730
20. Wolffe AP (1996) Histone deacetylase: a regulator of transcription. Science 272:371–372
21. Vega RB, Matsuda K, Oh J, Barbosa AC, Yang X, Meadows E, McAnally J, Pomajzl C, Shelton JM, Richardson JA, Karsenty G, Olson EN (2004) Histone deacetylase 4 controls chondrocyte hypertrophy during skeletogenesis. Cell 119:555–566
22. Sebastian C, Zwaans BM, Silberman DM, Gymrek M, Goren A, Zhong L, Ram O, Truelove J, Guimaraes AR, Toiber D, Cosentino C, Greenson JK, MacDonald AI, McGlynn L, Maxwell F, Edwards J, Giacosa S, Guccione E, Weissleder R, Bernstein BE, Regev A, Shiels PG, Lombard DB, Mostoslavsky R (2012) The histone deacetylase SIRT6 is a tumor suppressor that controls cancer metabolism. Cell 151:1185–1199
23. Hu E, Dul E, Sung CM, Chen Z, Kirkpatrick R, Zhang GF, Johanson K, Liu R, Lago A, Hofmann G, Macarron R, de los Frailes M, Perez P, Krawiec J, Winkler J, Jaye M (2003) Identification of novel isoform-selective inhibitors within class I histone deacetylases. J Pharmacol Exp Therap 307:720–728
24. Werner SL, Barken D, Hoffmann A (2005) Stimulus specificity of gene expression programs determined by temporal control of IKK activity. Science 309:1857–1861
25. Furia B, Deng L, Wu K, Baylor S, Kehn K, Li H, Donnelly R, Coleman T, Kashanchi F (2002) Enhancement of nuclear factor-κB acetylation by coactivator p300 and HIV-1 Tat proteins. J Biol Chem 277:4973–4980
26. Quivy V, Van Lint C (2004) Regulation at multiple levels of NF-κB-mediated transactivation by protein acetylation. Biochem Pharmacol 68:1221–1229
27. Hoberg JE, Yeung F, Mayo MW (2004) SMRT derepression by the IκB kinase alpha: a prerequisite to NF-κB transcription and survival. Mol Cell 16:245–255
28. Roth SY, Denu JM, Allis CD (2001) Histone acetyltransferases. Annu Rev Biochem 70:81–120
29. Vanden Berghe W, De Bosscher K, Boone E, Plaisance S, Haegeman G (1999) The nuclear factor-κB engages CBP/p300 and histone acetyltransferase activity for transcriptional activation of the interleukin-6 gene promoter. J Biol Chem 274:32091–32098
30. Kaina B, Christmann M, Naumann S, Roos WP (2007) MGMT: key node in the battle against genotoxicity, carcinogenicity and apoptosis induced by alkylating agents. DNA Rep 6:1079–1099
31. Suka N, Carmen AA, Rundlett SE, Grunstein M (1998) The regulation of gene activity by histones and the histone deacetylase RPD3. Cold Spring Harb Symp Quant Biol 63:391–399
32. Camphausen K, Burgan W, Cerra M, Oswald KA, Trepel JB, Lee MJ, Tofilon PJ (2004) Enhanced radiation-induced cell killing and prolongation of γH2AX foci expression by the histone deacetylase inhibitor MS-275. Cancer Res 64:316–321
33. Eyupoglu IY, Hahnen E, Trankle C, Savaskan NE, Siebzehnrubl FA, Buslei R, Lemke D, Wick W, Fahlbusch R, Blumcke I (2006) Experimental therapy of malignant gliomas using the inhibitor of histone deacetylase MS-275. Mol Cancer Ther 5:1248–1255
34. Palacios A, Garcia P, Padro D, Lopez-Hernandez E, Martin I, Blanco FJ (2006) Solution structure and NMR characterization of the binding to methylated histone tails of the plant homeodomain finger of the tumour suppressor ING4. FEBS Lett 580:6903–6908
35. Pena PV, Davrazou F, Shi X, Walter KL, Verkhusha VV, Gozani O, Zhao R, Kutateladze TG (2006) Molecular mechanism of histone H3K4me3 recognition by plant homeodomain of ING2. Nature 442:100–103
36. Gong W, Suzuki K, Russell M, Riabowol K (2005) Function of the ING family of PHD proteins in cancer. Int J Biochem Cell Biol 37:1054–1065

37. Campos EI, Chin MY, Kuo WH, Li G (2004) Biological functions of the ING family tumor suppressors. Cell Mol Life Sci 61:2597–2613
38. Shi X, Hong T, Walter KL, Ewalt M, Michishita E, Hung T, Carney D, Pena P, Lan F, Kaadige MR, Lacoste N, Cayrou C, Davrazou F, Saha A, Cairns BR, Ayer DE, Kutateladze TG, Shi Y, Cote J, Chua KF, Gozani O (2006) ING2 PHD domain links histone H3 lysine 4 methylation to active gene repression. Nature 442:96–99
39. Doyon Y, Cayrou C, Ullah M, Landry AJ, Cote V, Selleck W, Lane WS, Tan S, Yang XJ, Cote J (2006) ING tumor suppressor proteins are critical regulators of chromatin acetylation required for genome expression and perpetuation. Mol Cell 21:51–64
40. Shiseki M, Nagashima M, Pedeux RM, Kitahama-Shiseki M, Miura K, Okamura S, Onogi H, Higashimoto Y, Appella E, Yokota J, Harris CC (2003) p29ING4 and p28ING5 bind to p53 and p300, and enhance p53 activity. Cancer Res 63:2373–2378
41. Zhang X, Wang KS, Wang ZQ, Xu LS, Wang QW, Chen F, Wei DZ, Han ZG (2005) Nuclear localization signal of ING4 plays a key role in its binding to p53. Biochem Biophys Res Commun 331:1032–1038
42. Gunduz M, Nagatsuka H, Demircan K, Gunduz E, Cengiz B, Ouchida M, Tsujigiwa H, Yamachika E, Fukushima K, Beder L, Hirohata S, Ninomiya Y, Nishizaki K, Shimizu K, Nagai N (2005) Frequent deletion and down-regulation of ING4, a candidate tumor suppressor gene at 12p13, in head and neck squamous cell carcinomas. Gene 356:109–117